Materials Research Proceedings 31 (2023) 693-703 https://doi.org/10.21741/9781644902592-71

On the deformation of layered composite arches using exponential shear and normal deformation theory

Valmik M. Mahajan[1,a*] and Amit Sharma[2,b]

[1] Research Scholar, Department of Civil Engineering, Oriental University Indore-453555, Madhya Pradesh, India

[2] Professor, Department of Civil Engineering, Oriental University Indore-453555, Madhya Pradesh, India

[a]valmikmahajan001@gmail.com, [b]sgsitsamit25@gmail.com

Keywords: Deformation, Stresses, Displacements, Layered Composite Arches, ESNDT

Abstract. In the present study, the stresses and displacements are analyzed for layered composite arches of various lamination schemes subjected to uniformly loading. The present work is majorly highlighted the effects of transverse normal stress and transverse normal strain using exponential shear and normal deformation theory (ESNDT). Governing equations are derived using Hamilton's principle with application of Navier's method subjected to simply supported end conditions. Present theory is free from use of any shear correction factor and it satisfies the zero traction free end boundary condition at the top and bottom surfaces of the layered composite arches. In the present work symmetric and antisymmetric lamination scheme have been studied to obtain the numerical results for four layered composite arches and is validated through results available in prior literature.

Introduction

Composite arches are widely used across the world due to their exceptional qualities such as excellent strength, an admirable stiffness-to-weight ratio, and outstanding fatigue-resistance. Now a day, there is enormous demand in architectural view of the structures. Composite arches are most suitable for such innovative constructions. Hence, design of layered composite arches is very useful because of their superior properties compared to available materials. Subsequently, these composite materials are mostly used in mechanical and civil engineering, marine, automobile private sector, aerospace engineering, aircraft, ships, bridges and spacecraft. Curved and arched surfaces are commonly used in advanced architectural structures and military engineering for fighter jet, rocket launchers, antiballistic missiles, aircraft carriers, antitank-mines etc. The vast range of literature is available on straight beams/surfaces subjected to several loadings. Bernoulli-Euler [1, 2] established beam theory universally named as classical beam theory (CBT). But authors ignored the effect of thickness stretching. Further study has modified and improved by Timoshenko [3] with accounted the effect of shear deformation but it requires shear correction factor. These theories well-known as Timoshenko beam theory (TBT) or first order shear deformation (FSDT) theory in 1921. Classical and Timoshenko beam theory doesn't capture the transverse normal strain and shear deformation effects. In few decades, it is found that a very limited research is completed on arches or curved beams.

Reddy [4] has developed higher-order theory for composite-laminated plates and obtained results are validated through first-order-shear-deformation theory and 3-D elasticity solutions. Carrera [5] studied thermal-stress analysis for layered and isotropic (homogeneous) plates by adopting thickness stretching effect. Carrera *et al.* [6] addressed a model for static responses of FGM plates known as variable kinematic model subjected to mechanical loads. Zenkour [7] established the 3-D elasticity solution for sandwich and cross-ply laminates exposed to sinusoidally distributed (SDL) and uniformly distributed (UDL) loads. Kant and Shiyekar [8] presented model on cylindrical bending for piezoelectric-laminates plates using higher order theory. Tornabene [9] and his co-authors investigates the responses of static behavior for curved panels using DQM, differential geometry and Carrera-unified-formulation approach and also investigates recovery of repossession of stresses, shear-strains and transverse-normal through-the-thickness variations for functionally graded sandwich panels [10]. Sayyad and Ghugal [11] studied cylindrical bending for multilayered composite laminate plates using theory of higher-order. Present exponential shear and normal deformation theory captures excellent structural behavior of layered composite arches due to consideration of effect of transverse normal strain and transverse shear deformation. Present theory will be valuable asset in the research field of aerospace, civil and mechanical structures.

Mathematical-formulation for layered arches

Considered layered composite arches with one end is roller supported and another is hinged support with radius of curvature (*R*), for a length (*L*), total thickness (*h*) and unit width of the arch (*b*) $\{0 \le x \le L;\ -b/2 \le y \le b/2;\ -h/2 \le z \le h/2\}$ as shown in Fig. 1.

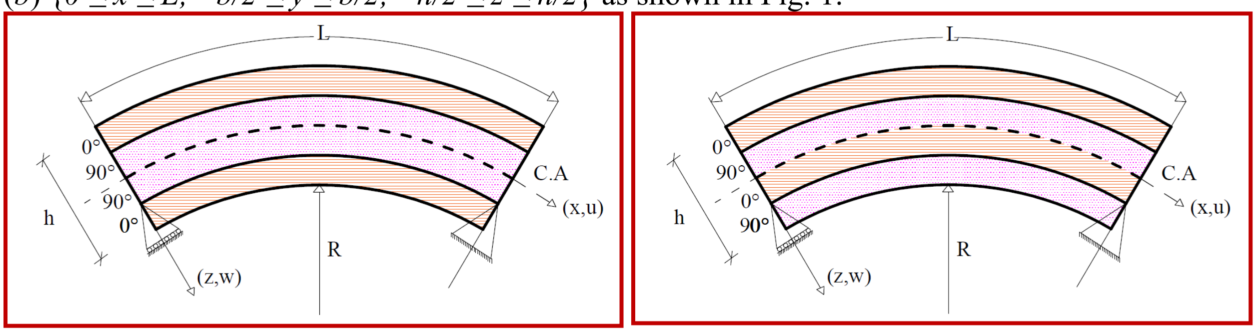

(a) Symmetric layered ($0^0/90^0/90^0/0^0$) arch (b) Antisymmetric layered ($0^0/90^0/0^0/90^0$) arch

Fig. 1 Geometry and coordinates system for layered composite arches

Displacement field

Displacement field for layered composite arches with consideration of transverse normal strain and shear deformations are given below,

$$u_{(x,z)} = \left(1+\frac{z}{R}\right)u_0 - z\frac{\partial w_0}{\partial x} + f(z)\phi \quad \text{and} \quad w_{(x,z)} = w_0 + f'(z)\psi\,. \tag{1}$$

Strain displacement relationship

$$\varepsilon_x^k = \left[\frac{\partial u}{\partial x} + \frac{w}{R}\right],\ \ \varepsilon_z^k = \left[\frac{\partial w}{\partial z}\right],\ \gamma_{xz}^k = \left[\frac{\partial u}{\partial z} + \frac{\partial w}{\partial x} - \frac{u_0}{R}\right]. \tag{2}$$

$$\varepsilon_x^k = \left[\frac{\partial u_0}{\partial x} - z\frac{\partial^2 w_0}{\partial x^2} + f(z)\frac{\partial \phi}{\partial x} + \frac{w_0}{R} + \frac{f'(z)}{R}\psi\right],\ \varepsilon_z^k = f''(z)\psi\,,\ \gamma_{xz}^k = f'(z)\left(\phi + \frac{\partial \psi}{\partial x}\right). \tag{3}$$

$$\text{where, } f(z) = z\,e^{-2\left(\frac{z}{h}\right)^2},\ f'(z) = e^{-2\left(\frac{z}{h}\right)^2}\left(1-\frac{4z^2}{h^2}\right),\ f''(z) = e^{-2\left(\frac{z}{h}\right)^2}\left(\frac{16z^3 - 12zh^2}{h^4}\right). \tag{4}$$

where, u_0, w_0, ϕ and ψ be the four unknown functions at mid-plane for composite arches. *f(z)* and *f'(z)* is shear and normal deformations. In present theory transverse normal strain is not equal to zero i.e. $\varepsilon_z \neq 0$. Shear deformation considered at any point on the arch as stated in Eq. (3).

Hooke's law

Two dimensional Hooke's law is applied layerwise to obtained equations for axial bending stresses and shear stresses with reference axes (*x,z*) from Eq. (5).

$$\begin{Bmatrix}\sigma_x\\ \sigma_z\\ \tau_{xz}\end{Bmatrix}^k = \begin{bmatrix}Q_{11} & Q_{13} & 0\\ Q_{13} & Q_{33} & 0\\ 0 & 0 & Q_{55}\end{bmatrix}^k \begin{Bmatrix}\varepsilon_x\\ \varepsilon_z\\ \gamma_{xz}\end{Bmatrix}^k \text{ or } \{\sigma\}^k = \left[Q_{ij}\right]^k \{\varepsilon\}^k. \tag{5}$$

where, $\{\sigma\}^k$ be normal stresses, $\{\varepsilon\}^k$ be transverse-shear-strain, and $\left[Q_{ij}\right]^k$ be transformed-rigidity-matrix w.r.t. (*x,z*) axes. Reduced stiffness coefficients are given below,

$$Q_{11}^k = \left[\frac{E_1^k}{1-(\mu_{13}*\mu_{31})}\right],\ Q_{13}^k = \left[\frac{E_3^k*\mu_{13}}{1-(\mu_{13}*\mu_{31})}\right],\ Q_{33}^k = \left[\frac{E_3^k}{1-(\mu_{13}*\mu_{31})}\right],\ Q_{44}^k = G_{23}^k,\ Q_{55}^k = G_{13}^k. \tag{6}$$

where, μ_{13} and μ_{31} be the Poisson's ratio, E_1^k and E_3^k are elasticity-modulus about (*x,z*) axes and G_{13}^k and G_{23}^k are the shear-modulus. Axial-bending stresses is stated as per Hooke's law,

$$\sigma_x^k = Q_{11}^k\,\varepsilon_x^k + Q_{13}^k\,\varepsilon_z^k,\ \sigma_z^k = Q_{13}^k\,\varepsilon_x^k + Q_{33}^k\,\varepsilon_z^k,\ \tau_{xz}^k = Q_{55}^k\,\gamma_{xz}^k,\ \varepsilon_y^k = \gamma_{xy}^k = \gamma_{yz}^k = 0. \tag{7}$$

Hamilton's principle

Using virtual work principle with application of integration by-parts for traction free simply supported boundary condition are given below, where, (δ) called as variational-operator. The complete expression for Eq. (8) generated from Eq. (2). we have,

$$\therefore \int_0^L \int_{-h/2}^{+h/2} \left(\sigma_x^k\,\delta\varepsilon_x + \sigma_z^k\,\delta\varepsilon_z + \tau_{xz}^k\,\delta\gamma_{xz}\right)dx\,dz - \int_0^L \left(q\,\delta w\,dx\right) = 0. \tag{8}$$

$$\begin{aligned}\int_{-h/2}^{+h/2}\int_0^L \left(\sigma_x^k\,\delta\varepsilon_x\right)dx\,dz = \int_{-h/2}^{+h/2}\int_0^L &\left[Q_{11}\left(\frac{\partial u_0}{\partial x} - z\frac{\partial^2 w_0}{\partial x} + f(z)\frac{\partial\phi}{\partial x} + \frac{w_0}{R} + \frac{f'(z)}{R}\psi\right) + Q_{13}\left(f''(z)\right)\psi\right]\\ &*\left[\frac{\partial\delta u_0}{\partial x} - z\frac{\partial^2\delta w_0}{\partial x} + f(z)\frac{\partial\delta\phi}{\partial x} + \frac{\delta w_0}{R} + \frac{f'(z)}{R}\delta\psi\right]dx\,dz\end{aligned}. \tag{9}$$

$$\int_{-h/2}^{+h/2}\int_0^L \left(\sigma_z^k\,\delta\varepsilon_z\right)dx\,dz = \int_{-h/2}^{+h/2}\int_0^L \left\{\begin{bmatrix}Q_{13}\left(\frac{\partial u_0}{\partial x} - z\frac{\partial^2 w_0}{\partial x} + f(z)\frac{\partial\phi}{\partial x} + \frac{w_0}{R} + \frac{f'(z)}{R}\psi\right)\\ +Q_{33}\left(f''(z)\right)\psi\end{bmatrix}*\left[f''(z)\,\delta\psi\right]\right\}dx\,dz. \tag{10}$$

$$\int_{-h/2}^{+h/2}\int_0^L \left(\tau_{xz}^k\,\delta\gamma_{xz}\right)dx\,dz = \int_{-h/2}^{+h/2}\int_0^L \left\{\left[Q_{55}\,f'(z)\left(\phi + \frac{\partial\psi}{\partial x}\right)\right]*\left[f'(z)\left(\delta\phi + \frac{\partial\delta\psi}{\partial x}\right)\right]\right\}dx\,dz. \tag{11}$$

From Eq. (9) - (11) integrate individuals one by one and solve the expression by-parts rule and finally gathering the terms of δu_0, δw_0, $\delta\phi$ and $\delta\psi$ to build governing equations.

$$\begin{bmatrix}A_{11}, B_{11}, C_{11}, D_{11}, E_{11}, F_{11}\\ G_{11}, H_{11}, I_{11}, J_{11}\end{bmatrix} = Q_{11}^k \int_{-h/2}^{+h/2} \begin{bmatrix}1, z, f(z), f'(z), z^2, z\,f(z)\\ z\,f'(z), f(z)^2, f(z)\,f'(z), f'(z)^2\end{bmatrix} dz. \tag{12}$$

$$\left[L_{13}, M_{13}, N_{13}, O_{13}\right] = Q_{13}^k \int_{-h/2}^{+h/2} \left[f''(z), z\,f''(z), f(z)\,f''(z), f'(z)\,f''(z)\right] dz. \tag{13}$$

$$[L_{33}]=Q_{33}^k \int_{-h/2}^{+h/2}\left[f''(z)^2\right]dz\,,[J_{55}]=Q_{55}^k \int_{-h/2}^{+h/2}\left[f'(z)^2\right]dz\,. \tag{14}$$

Governing equation achieved in the normalized form with integration constants are listed below from Eq. (15) to Eq. (18).

$$\delta u_0: -A_{11}\left(\frac{\partial^2 u_0}{\partial x^2}\right)+B_{11}\left(\frac{\partial^3 w_0}{\partial x^3}\right)-\frac{A_{11}}{R}\left(\frac{\partial w_0}{\partial x}\right)-C_{11}\left(\frac{\partial^2 \phi}{\partial x^2}\right)-\left(\frac{D_{11}}{R}+L_{13}\right)\left(\frac{\partial \psi}{\partial x}\right)=0\,. \tag{15}$$

$$\begin{aligned}\delta w_0: &-B_{11}\left(\frac{\partial^3 u_0}{\partial x^3}\right)+\frac{A_{11}}{R}\left(\frac{\partial u_0}{\partial x}\right)+E_{11}\left(\frac{\partial^4 w_0}{\partial x^4}\right)-2\frac{B_{11}}{R}\left(\frac{\partial^2 w_0}{\partial x^2}\right)+\frac{A_{11}}{R^2}\left(w_0\right)-F_{11}\left(\frac{\partial^3 \phi}{\partial x^3}\right)+\frac{C_{11}}{R}\left(\frac{\partial \phi}{\partial x}\right)\\ &+\left(\frac{D_{11}}{R^2}+\frac{L_{13}}{R}\right)(\psi)-\left(\frac{G_{11}}{R}+M_{13}\right)\left(\frac{\partial^2 \psi}{\partial x^2}\right)=q_0\end{aligned}\,. \tag{16}$$

$$\begin{aligned}\delta\phi: &-C_{11}\left(\frac{\partial^2 u_0}{\partial x^2}\right)+F_{11}\left(\frac{\partial^3 w_0}{\partial x^3}\right)-\frac{C_{11}}{R}\left(\frac{\partial w_0}{\partial x}\right)+J_{55}\,\phi-H_{11}\left(\frac{\partial^2 \phi}{\partial x^2}\right)-\frac{I_{11}}{R}\left(\frac{\partial \psi}{\partial x}\right)-N_{13}\left(\frac{\partial \psi}{\partial x}\right)\\ &+J_{55}\left(\frac{\partial \psi}{\partial x}\right)=0\end{aligned}\,. \tag{17}$$

$$\begin{aligned}\delta\psi: &\left(\frac{D_{11}}{R}+L_{13}\right)\left(\frac{\partial u_0}{\partial x}\right)+\left(\frac{D_{11}}{R^2}+\frac{L_{13}}{R}\right)w_0-\left(\frac{G_{11}}{R}+M_{13}\right)\left(\frac{\partial^2 w_0}{\partial x^2}\right)+\frac{I_{11}}{R}\left(\frac{\partial \phi}{\partial x}\right)+N_{13}\left(\frac{\partial \phi}{\partial x}\right)\\ &-J_{55}\left(\frac{\partial \phi}{\partial x}\right)+\frac{J_{11}}{R}\psi+2\frac{O_{13}}{R}\psi+L_{33}\,\psi-J_{55}\left(\frac{\partial^2 \psi}{\partial x^2}\right)=0\end{aligned}\,. \tag{18}$$

Navier's method
This technique is applied for simply supported (SS) boundary condition for layered composite arch under the action of transverse uniformly distributed loading (UDL).

$$u_0 = w_0 = \phi = \psi = 0, \text{ at } x = L, x = 0\,. \tag{19}$$

In the form of trigonometric, unknown variables are listed below,

$$u_0=\sum_{m=1}^{\infty} u_m \cos(\alpha x),\; w_0=\sum_{m=1}^{\infty} w_m \sin(\alpha x),\; \phi=\sum_{m=1}^{\infty}\phi_m \cos(\alpha x),\; \psi=\sum_{m=1}^{\infty}\psi_m \sin(\alpha x) \tag{20}$$

$$q_0 = q_m \sin(\alpha x), \qquad \left(\because \alpha = {}^{m\pi}\!/_{L}\right). \tag{21}$$

where, u_m, w_m, ϕ_m and ψ_m be the unknown-factors. Transverse UDL as stated below,

$$q_{(x)}=\sum_{m=1}^{\infty}\left(\frac{4\,q_0}{m\,\pi}\sin(\alpha x)\right)\,. \tag{22}$$

where, *m*=Positive integer-variables from odd numbers to the infinity (∞). Substituting the values of unit loading from Eq. (22) and, (u, w, ϕ, ψ) unknown variables of Eq. (20) and Eq. (21) by putting in the governing equations. Bending stresses for layered composite arches are presented in matrix form of Eq. (23) is given below.

$$[K]\{\Delta\}=\{f\} \text{ or } \begin{bmatrix} K_{11} & K_{12} & K_{13} & K_{14} \\ K_{21} & K_{22} & K_{23} & K_{24} \\ K_{31} & K_{32} & K_{33} & K_{34} \\ K_{41} & K_{42} & K_{43} & K_{44} \end{bmatrix} \begin{Bmatrix} u_m \\ w_m \\ \phi_m \\ \psi_m \end{Bmatrix} = \begin{Bmatrix} 0 \\ q_m \\ 0 \\ 0 \end{Bmatrix}. \tag{23}$$

where, $[K]$= known as stiffness-matrix; $\{\Delta\}$= called as unknown-variables and $\{f\}$= known as force-vector. The each elements of stiffness matrix are stated below,

$$K_{11}=A_{11}\alpha^2 \quad K_{12}=-\left(\frac{A_{11}}{R}\alpha+B_{11}\alpha^3\right) \quad K_{13}=C_{11}\alpha^2 \quad K_{14}=-\left(\frac{D_{11}}{R}\alpha+L_{13}\alpha\right)$$

$$K_{21}=K_{12} \quad K_{22}=\left(\frac{A_{11}}{R^2}+2\frac{B_{11}}{R}\alpha^2+E_{11}\alpha^4\right) \quad K_{23}=-\left(\frac{C_{11}}{R}\alpha+F_{11}\alpha^3\right) \quad K_{24}=\left(\frac{D_{11}}{R^2}+\frac{L_{13}}{R}\right)+\left(\frac{G_{11}}{R}\alpha^2+M_{13}\alpha^2\right)$$

$$K_{31}=K_{13} \quad K_{32}=K_{23} \quad K_{33}=\left(H_{11}\alpha^2+J_{55}\right) \quad K_{34}=-\left(\frac{I_{11}}{R}\alpha+N_{13}\alpha-J_{55}\alpha\right)$$

$$K_{41}=K_{42} \quad K_{42}=K_{24} \quad K_{43}=K_{34} \quad K_{44}=\left(\frac{J_{11}}{R^2}+2\frac{O_{13}}{R}+L_{33}+J_{55}\alpha^2\right)$$

Present theory considered the normalized displacements and stresses relation are given below,

$$\bar{w}=\frac{100E_3h^3}{q_0L^4}w\left(\frac{L}{2},0\right),\ \bar{u}=\frac{E_3}{q_0h}u\left(0,-\frac{h}{2}\right),\ \bar{\sigma}_x=\frac{h}{q_0}\sigma_x\left(\frac{L}{2},-\frac{h}{2}\right),\ \bar{\tau}_{xz}=\frac{\tau_{xz}}{q_0}(0,0). \tag{24}$$

where $\bar{w}$, $\bar{u}$, $\bar{\sigma}_x$ and $\bar{\tau}_{xz}$ be dimensionless parameters.

Numerical results with discussions

Numerical results are presented in tabular form consists of Table 2 to Table 5 and variations of displacements and stresses for layered composite arches through the thickness are plotted using Grapher as shown in Figure 2 to Figure 5. Present theory analyzed the different lamination schemes for arches viz, symmetric and antisymmetric layered composite arches. The material properties for various arches are given below in Table 1.

Table 1 Materials property for layered composite arches.

Theory	Source	Lamination scheme	Properties
Present	Sayyad and Ghugal [11]	$(0^0/90^0/90^0/0^0)$ symmetric arch	E_1 =181 GPa; E_3 =10.3 GPa; G_{13} =7.17 GPa; G_{23} =2.87 GPa; μ_{13} =0.25; μ_{31} =0.01.
		$(0^0/90^0/0^0/90^0)$ antisymmetric arch	E_1=172.5 GPa; E_3=6.9 GPa; G_{13}=3.45 GPa; G_{23}=1.38 GPa; μ_{13} =0.25; μ_{31} =0.01.

Table 2 presented the non-dimensional results for four layered symmetric straight beams when subjected to transverse uniformly distributed loadings. Present results are in good-agreement with earlier published results by Sayyad and Ghugal [11] of normalized stresses and displacements for aspect ratio *L/h* = 4, 10 and 100. Present numerical results are compared and closely matches with well-known theory of Reddy [4] for transverse and axial deformation at aspect ratio *L/h* = 100.

Normalized axial displacements and transverse deflections are plotted through the thickness of symmetric layered composite arch as shown in Figure 2. With the application of constitutive relation, it is observed that at the interlaminar surfaces of arches shows two values for shear stress and axial bending through the thickness as shown in Figure 3 for symmetric layered and Figure 5 for antisymmetric layered composite arch.

Table 2 Normalized displacements and stresses for four layered ($0^0/90^0/90^0/0^0$) straight beams.

Theory	L/h	Model	$\bar{w}$ (L/2,0)	$\bar{u}$ (0,-h/2)	$\bar{\sigma}_x$ (L/2,-h/2)	$\bar{\tau}_{xz}$ (0,0)
Present ($\varepsilon_z \neq 0$)		ESNDT	3.4548	1.4850	18.1369	2.1863
Sayyad and Ghugal [11]		SSNPT	3.4354	1.4648	17.9237	2.3734
Reddy [4]	4	HSDT	3.4033	1.4401	17.6119	2.3250
Timoshenko [3]		FSDT	2.6074	1.0285	13.6041	2.5586
Bernoulli-Euler [1,2]		CBT	1.0044	1.0285	13.6041	2.5586
Present ($\varepsilon_z \neq 0$)		ESNDT	1.4073	17.3079	89.4987	5.9314
Sayyad and Ghugal [11]		SSNPT	1.3986	17.1903	89.3921	6.0174
Reddy [4]	10	HSDT	1.3939	17.1607	89.0567	6.0575
Timoshenko [3]		FSDT	1.2609	16.0703	85.0255	6.3965
Bernoulli-Euler [1,2]		CBT	1.0044	16.0703	85.0255	6.3965
Present ($\varepsilon_z \neq 0$)		ESNDT	1.0091	16094.00	8499.900	62.0397
Sayyad and Ghugal [11]		SSNPT	1.0057	16039.93	8509.589	63.8913
Reddy [4]	100	HSDT	1.0084	16082.14	8507.056	63.9154
Timoshenko [3]		FSDT	1.0069	16070.26	8502.562	63.9646
Bernoulli-Euler [1,2]		CBT	1.0044	16070.26	8502.562	63.9646

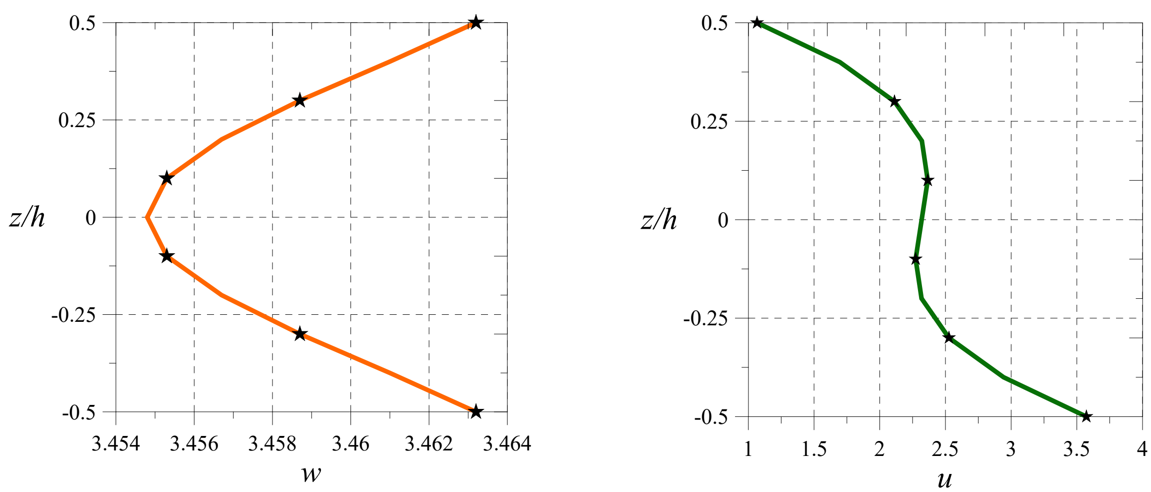

Fig. 2 Normalized transverse and axial deformations through-the-thickness for four layered symmetric ($0^0/90^0/90^0/0^0$) composite arch due to uniformly distributed loading [R/h =5, L/h =4].

Table 3 presented the normalized transverse ($\bar{w}$) deformation, axial ($\bar{u}$) deformation, axial bending stress ($\bar{\sigma}_x$) and shear stress ($\bar{\tau}_{xz}$) deformation for four-layered symmetric composite arch subjected to uniformly loading for aspect ratio (L/h = 4, 10, 100). It is observed that, maximum non-dimensional value of axial deformation and axial bending stress have noted at the top fibre of layered arch i.e. ($z/h = -h/2$) due to placing of fibers in 0^0 horizontal direction along the length of arches. While minimum non-dimensional bending stress and axial displacement have been reported at bottom surface of the arch i.e. ($z/h = +h/2$), it means that fibers are laid in 90^0 direction or perpendicular to zero degree layer of the arch. From Table 3 it is observed that transverse deflection and shear stress deformation remains constants with varying radius of curvature. Table 4 presented numerical results of stresses and displacements for four-layered antisymmetric composite arch. It is found that normalized shear stress and transverse deflection are remains constant with varying radius of curvature for aspect ratio L/h = 4, 10, 100 (R/h = 1.0 to ∞).

Materials Research Proceedings 31 (2023) 693-703 https://doi.org/10.21741/9781644902592-71

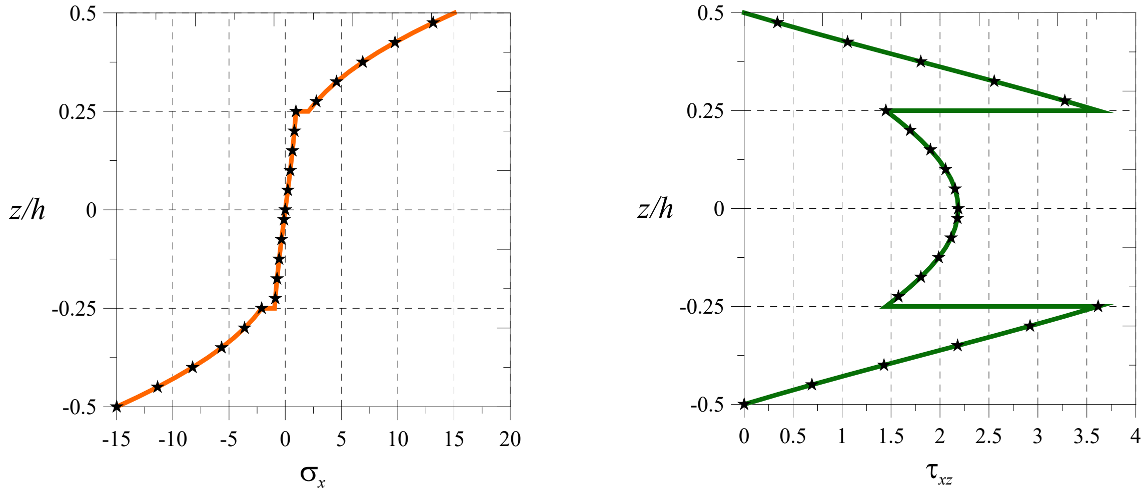

Fig. 3 Normalized axial-bending and shear stresses through-the-thickness for four layered symmetric ($0^0/90^0/90^0/0^0$) composite arch due to uniformly distributed loading [R/h =5, L/h =4].

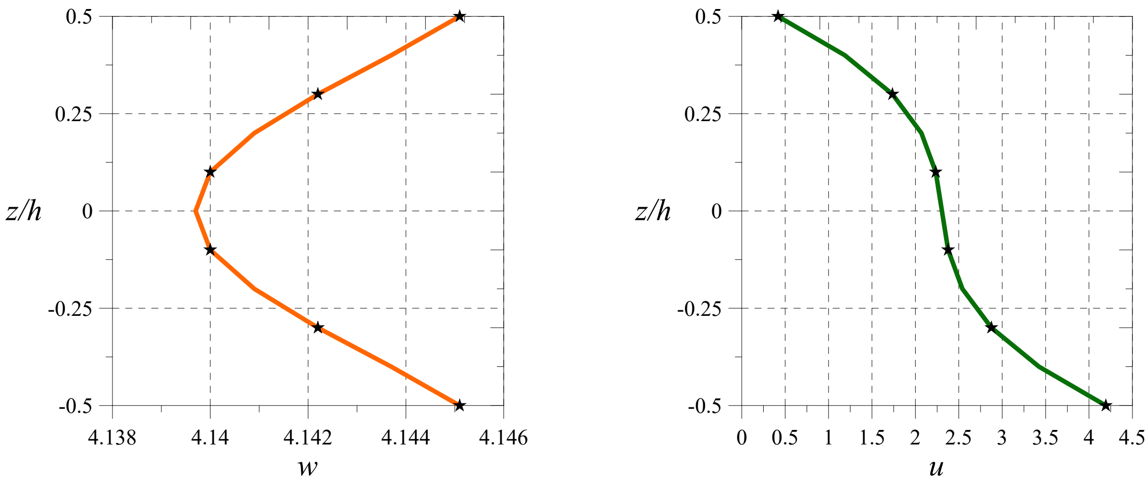

Fig. 4 Normalized transverse and axial deformations through-the-thickness for four layered antisymmetric ($0^0/90^0/0^0/90^0$) composite arch due to uniformly distributed loading [R/h=5,L/h=4]

It is observed that the variations of bending stress through the thickness is nearly equal to zero when the fibers are placed in 90^0 direction of 2nd and 4th layer of antisymmetric composite arch under the action of transverse uniformly distributed loading as shown in Figure 5. It is also observed that bending stress is increasing parabolically in 1st layer from maximum non-dimensional to zero and 3rd layer varying from minimum to maximum non-dimensional of the layered arch. But in case of shear stress is linearly increasing in the 1st layer, parabolic nature in 2nd and 3rd layer and nearly equal to zero variations in the 4th layer of four layered antisymmetric composite arch subjected to uniformly loading through the thickness variations.

Table 5 shows that, present theory have been great-agreement to Sayyad and Ghugal [11] for stresses and displacements at aspect ratio (*L/h* = 10). Present numerical results of transverse deformation are closely-matches with well-known theory of Reddy [4] at aspect ratio (*L/h* = 4, 10 and 100). In the present investigation it is found that transverse shear stress is slightly improved for aspect ratio (*L/h* = 4, 10 and 100). Present theory well captures the effect of normal deformation

Materials Research Proceedings 31 (2023) 693-703 https://doi.org/10.21741/9781644902592-71

which is not considered in some prior available literature and numerical results are exceptional matches with Sayyad and Ghugal [11] and Reddy [4].

Table 3 Normalized displacements and stresses for four layered symmetric composite arch.

Theory	L/h	R/h	$\bar{w}$ (L/2,0)	$\bar{u}$ (0,-h/2)	$\bar{\sigma}_x$ (L/2,-h/2)	$\bar{\tau}_{xz}$ (0,0)
Present ($\varepsilon_z \neq 0$)	4	1	3.4549	7.2830	60.0227	2.1865
Present ($\varepsilon_z \neq 0$)		2	3.4548	5.8335	1.4377	2.1864
Present ($\varepsilon_z \neq 0$)		3	3.4548	4.7061	9.4218	2.1864
Present ($\varepsilon_z \neq 0$)		4	3.4548	4.0216	13.2260	2.1864
Present ($\varepsilon_z \neq 0$)		5	3.4548	3.5723	14.9884	2.1864
Present ($\varepsilon_z \neq 0$)		10	3.4548	2.5866	17.3429	2.1863
Present ($\varepsilon_z \neq 0$)		25	3.4548	1.9395	18.0065	2.1863
Present ($\varepsilon_z \neq 0$)		50	3.4548	1.7146	18.1029	2.1863
Present ($\varepsilon_z \neq 0$)		100	3.4548	1.6003	18.1277	2.1863
Present ($\varepsilon_z \neq 0$)		∞	3.4548	1.4850	18.1369	2.1863
Present ($\varepsilon_z \neq 0$)	10	1	1.4073	244.9949	1149.700	5.9316
Present ($\varepsilon_z \neq 0$)		2	1.4073	188.0736	220.2640	5.9315
Present ($\varepsilon_z \neq 0$)		3	1.4073	143.8010	48.1529	5.9314
Present ($\varepsilon_z \neq 0$)		4	1.4073	116.9212	12.0813	5.9314
Present ($\varepsilon_z \neq 0$)		5	1.4073	99.2755	39.9590	5.9314
Present ($\varepsilon_z \neq 0$)		10	1.4073	60.5685	77.1231	5.9314
Present ($\varepsilon_z \neq 0$)		25	1.4073	35.1586	87.5231	5.9314
Present ($\varepsilon_z \neq 0$)		50	1.4073	26.3243	89.0066	5.9314
Present ($\varepsilon_z \neq 0$)		100	1.4073	21.8388	89.3766	5.9314
Present ($\varepsilon_z \neq 0$)		∞	1.4073	17.3079	89.4987	5.9314
Present ($\varepsilon_z \neq 0$)	100	1	1.0091	1.6164E+7	8.8801E+6	62.0398
Present ($\varepsilon_z \neq 0$)		2	1.0091	1.2127E+7	2.2137E+6	62.0397
Present ($\varepsilon_z \neq 0$)		3	1.0091	8.9875E+6	9.7912E+5	62.0397
Present ($\varepsilon_z \neq 0$)		4	1.0091	7.0811E+6	5.4704E+5	62.0397
Present ($\varepsilon_z \neq 0$)		5	1.0091	5.8296E+6	3.4704E+5	62.0397
Present ($\varepsilon_z \neq 0$)		10	1.0091	3.0843E+6	8.0384E+4	62.0397
Present ($\varepsilon_z \neq 0$)		25	1.0091	1.2821E+6	5720.6000	62.0397
Present ($\varepsilon_z \neq 0$)		50	1.0091	6.5558E+5	4945.2000	62.0397
Present ($\varepsilon_z \neq 0$)		100	1.0091	3.3745E+5	7611.4000	62.0397
Present ($\varepsilon_z \neq 0$)		∞	1.0091	16094.000	8499.9000	62.0397

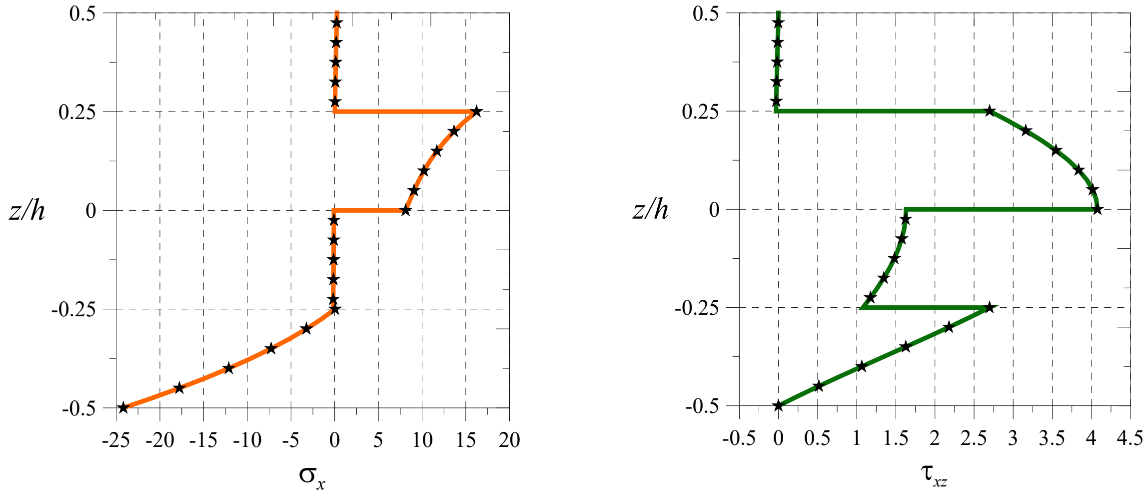

Fig. 5 Normalized axial-bending and shear stresses through-the-thickness for four layered antisymmetric ($0^0/90^0/0^0/90^0$) composite arch due to uniformly distributed loading [R/h=5,L/h=4]

Table 4 Normalized displacements and stresses for four layered antisymmetric composite arch.

Theory	L/h	R/h	$\bar{w}$ (L/2,0)	$\bar{u}$ (0,-h/2)	$\bar{\sigma}_x$ (L/2,-h/2)	$\bar{\tau}_{xz}$ (0,0)
Present ($\varepsilon_z \neq 0$)		1	4.1602	8.8736	101.0799	4.0791
Present ($\varepsilon_z \neq 0$)		2	4.1441	6.9762	2.5958	4.0781
Present ($\varepsilon_z \neq 0$)		3	4.1412	5.5826	15.2512	4.0780
Present ($\varepsilon_z \neq 0$)		4	4.1402	4.7432	21.3900	4.0780
Present ($\varepsilon_z \neq 0$)	4	5	4.1397	4.1939	24.1841	4.0780
Present ($\varepsilon_z \neq 0$)		10	4.1391	2.9924	27.7744	4.0781
Present ($\varepsilon_z \neq 0$)		25	4.1390	2.2056	28.6508	4.0781
Present ($\varepsilon_z \neq 0$)		50	4.1390	1.9323	28.7301	4.0781
Present ($\varepsilon_z \neq 0$)		100	4.1390	1.7936	28.7298	4.0782
Present ($\varepsilon_z \neq 0$)		∞	4.1390	1.6535	28.7030	4.0782
Present ($\varepsilon_z \neq 0$)		1	1.8864	326.7604	2205.500	11.1041
Present ($\varepsilon_z \neq 0$)		2	1.8745	247.5209	437.7593	11.1005
Present ($\varepsilon_z \neq 0$)		3	1.8727	187.9800	114.4785	11.1000
Present ($\varepsilon_z \neq 0$)		4	1.8723	151.9904	2.0108	11.0999
Present ($\varepsilon_z \neq 0$)	10	5	1.8721	128.4004	49.7849	11.0998
Present ($\varepsilon_z \neq 0$)		10	1.8721	76.71360	118.1390	11.0999
Present ($\varepsilon_z \neq 0$)		25	1.8723	42.80650	136.6160	11.0999
Present ($\varepsilon_z \neq 0$)		50	1.8724	31.01990	139.0198	11.1000
Present ($\varepsilon_z \neq 0$)		100	1.8724	25.03570	139.5175	11.1000
Present ($\varepsilon_z \neq 0$)		∞	1.8725	18.99070	139.5457	11.1000
Present ($\varepsilon_z \neq 0$)		1	1.4431	2.3113E+7	1.8069E+7	116.3519
Present ($\varepsilon_z \neq 0$)		2	1.4321	1.7206E+7	4.4723E+6	116.3114
Present ($\varepsilon_z \neq 0$)		3	1.4305	1.2736E+7	1.9779E+6	116.3044
Present ($\varepsilon_z \neq 0$)	100	4	1.4301	1.0030E+7	1.1064E+6	116.3022
Present ($\varepsilon_z \neq 0$)		5	1.4300	8.2561E+6	7.0321E+5	116.3013
Present ($\varepsilon_z \neq 0$)		10	1.4301	4.3660E+6	1.6581E+5	116.3003
Present ($\varepsilon_z \neq 0$)		25	1.4304	1.8121E+6	1.5397E+4	116.3003
Present ($\varepsilon_z \neq 0$)		50	1.4305	9.2408E+5	6071.9000	116.3004

Present ($\varepsilon_z \neq 0$)	100	1.4305	4.7313E+5	11430.000	116.3005
Present ($\varepsilon_z \neq 0$)	∞	1.4306	17567.000	13203.000	116.3005

Table 5 Normalized displacements and stresses for four layered ($0^0/90^0/0^0/90^0$) straight beams.

Theory	*L/h*	Model	$\bar{w}$ *(L/2,0)*	$\bar{u}$ *(0,-h/2)*	$\bar{\sigma}_x$ *(L/2,-h/2)*	$\bar{\tau}_{xz}$ *(0,0)*
Present ($\varepsilon_z \neq 0$)		ESNDT	4.1390	1.6535	28.7030	4.0782
Sayyad and Ghugal [11]		SSNPT	4.1737	1.6454	28.4633	3.7133
Reddy [4]	4	HSDT	4.1744	1.6222	28.0294	3.6618
Timoshenko [3]		FSDT	4.1055	1.1239	21.1274	3.5289
Bernoulli-Euler [1,2]		CBT	1.4269	1.1267	21.1274	3.5289
Present ($\varepsilon_z \neq 0$)		ESNDT	1.8725	18.9907	139.5457	11.1000
Sayyad and Ghugal [11]		SSNPT	1.8722	18.9205	139.4595	8.48720
Reddy [4]	10	HSDT	1.8731	18.8824	138.9880	8.50550
Timoshenko [3]		FSDT	1.8555	17.5615	132.0461	8.82230
Bernoulli-Euler [1,2]		CBT	1.4269	17.6055	132.0461	8.82230

Table 5 continued.....

Present ($\varepsilon_z \neq 0$)		ESNDT	1.4306	17567.00	13203.00	116.3005
Sayyad and Ghugal [11]		SSNPT	1.4286	17540.51	13216.65	88.18290
Reddy [4]	100	HSDT	1.4314	17575.30	13211.91	88.17670
Timoshenko [3]		FSDT	1.4312	17561.83	13204.90	88.22490
Bernoulli-Euler [1,2]		CBT	1.4269	17605.47	13204.61	88.22490

Conclusions

Present scientific study mainly contributes the precise exponential shear and normal deformation theory for symmetric and antisymmetric four-layered composite arches when subjected to uniform load. The effects of transverse normal-stress and transverse normal-strain have been taken into account by present theory. The present theory meets the zero traction free end boundary condition and does not require any shear correction factors. Present theory is very accurate estimation for displacements and stresses which are rarely found in the literature. The obtained numerical results can be use for accurate design of such complex engineering structures. These innovative results will obviously set the benchmark for upcoming researchers in the area of composite arches.

References

[1] J. Bernoulli, Curvatura laminae elasticae, Acta Eruditorum Lipsiae. 34 (1694) 262-276.

[2] L. Euler, Methodus inveniendi lineas curvas maximi minimive proprietate gaudentes, Apud Marcum-Michaelem Bousquet and Socios. 24 (1744) 1-322. https://doi.org/10.5479/sil.318525.39088000877480.

[3] S.P. Timoshenko, On the correction for shear of the differential equation for transverse vibrations of prismatic bars, Philos. Mag. Series 1. 41 (1921) 744-746. https://doi.org/10.1080/14786442108636264.

[4] J.N. Reddy, A simple higher-order theory for laminated composite plates, J. Appl. Mech. 51(4) (1984) 745-752. https://doi.org/10.1115/1.3167719.

[5] E. Carrera, Transverse normal strain effects on thermal stress analysis of homogeneous and layered plates, AIAA J. 43(10) (2005) 2232-2242. https://doi.org/10.2514/1.11230.

[6] E. Carrera, S. Brischetto and A. Robaldo, Variable kinematic model for the analysis of functionally graded material plates, AIAA J. 46(1) (2008) 194-203.

https://doi.org/10.2514/1.32490.

[7] A.M. Zenkour, Three-dimensional elasticity solution for uniformly loaded cross-ply laminates and sandwich plates, J. Sandw. Struct. Mater. 9(3) (2007) 213-238. https://doi.org/10.1177/1099636207065675.

[8] T. Kant and S.M. Shiyekar, Cylindrical bending of piezoelectric laminates with a higher order shear and normal deformation theory, Comput. Struct. 86 (2008) 1594-1603. https://doi.org/10.1016/j.compstruc.2008.01.002.

[9] F. Tornabene, N. Fantuzzi, E. Viola and E. Carrera, Static analysis of doubly-curved anisotropic shells and panels using CUF approach, differential geometry and differential quadrature method, Compos. Struct. 107 (2014) 675-697. http://dx.doi.org/10.1016/j.compstruct.2013.08.038.

[10] F. Tornabene, N. Fantuzzi, E. Viola and R.C. Batra, Stress and strain recovery for functionally graded free-form and doubly-curved sandwich shells using higher-order equivalent single layer theory, Compos. Struct. 119 (2015) 67-89. http://dx.doi.org/10.1016/j.compstruct.2014.08.005.

[11] A.S. Sayyad and Y.M. Ghugal, Cylindrical bending of multilayered composite laminates and sandwiches, Adv. Aircr. Spacecr. Sci. 3(2) (2016) 113-148. http://dx.doi.org/10.12989/aas.2016.3.2.113.